Angewandte Chemie

DOI: 10.1002/anie.200603553

Molecular Dynamics

Mechanisms of the Elementary Processes of Electron Wavepacket Dynamics Coupled with Proton Transfer and Hydrogen-Atom Migration in $H_2O + H_3O^+$**

*Hiroshi Ushiyama and Kazuo Takatsuka**

The dynamics of the coupled transfer of electrons and protons (or hydrogen atoms) are very important for the understanding of elementary processes in many fields of science.[1–10] A typical example of coupling between proton transfer and electron flow in a molecule is tautomerization, the static view of which is widely known in organic chemistry. As a dynamical consequence, proton transfer in 5-methyltropolone has been found to induce internal rotation of the methyl group at a remote site, which is mediated by coupling between the resultant tautomerization and hyperconjugation of the methyl group[9] (see also references [7,8]). It thus turns out that electron flow coupled with proton transfer induces deterministic dynamics, which contrast markedly with stochastic dynamics due to the intramolecular redistribution of vibrational energy. These examples and many others suggest that it is important to study the mechanism of coupled (simultaneous) motion of protons (or hydrogen atoms) and electron wavepackets not only for its own sake but also because of the recent progress of laser technology towards the attosecond ($1\ \mathrm{as} = 10^{-18}\ \mathrm{s}$) timescale.[11–14]

We present herein a study on the dynamics in $H_2O + H_3O^+$, a prototypical proton-transfer reaction, by the semiclassical Ehrenfest method, which tracks real-time quantum electron wavepacket propagation coupled with classical nuclear motions.[15–17] We survey two prototypes of proton transfer and hydrogen-atom migration, the distinction of which is often controversial in the practical analysis of experimental and theoretical studies.[18–20]

We first outline the semiclassical (mean-field) Ehrenfest method.[21–23] Those who are not interested in the theoretical method may skip this paragraph. The molecular electron wavepacket is expanded in terms of the Slater determinants and/or configuration state functions (CSF) [Eq (1)] and the

$$\Phi(\boldsymbol{r},t;\boldsymbol{R}(t)) = \sum_I C_I(t)\Phi_I(\boldsymbol{r};\boldsymbol{R})|_{\boldsymbol{R}=\boldsymbol{R}(t)} \qquad (1)$$

time-dependent coefficients $C_I(t)$ are to be determined with the electronic Schrödinger equation (2) where H^{el} is the

$$i\hbar\frac{\partial}{\partial t}\Phi(\boldsymbol{r},t;\boldsymbol{R}(t)) = H^{\mathrm{el}}(\boldsymbol{r};\boldsymbol{R}(t))\Phi(\boldsymbol{r},t;\boldsymbol{R}(t)) \qquad (2)$$

electronic Hamiltonian in the electronic coordinates $\boldsymbol{r}$. These quantum electron dynamics are coupled with classical nuclear motions $\boldsymbol{R}(t)$. "Classical forces" acting on the nuclei are given in Equation (3), where $\ddot{\boldsymbol{R}}_k(t)$ and M_k are acceleration and the

$$M_k\ddot{\boldsymbol{R}}_k(t) = -\sum_{IJ} C_I^*\frac{\partial H^{\mathrm{el}}_{IJ}}{\partial R_k}C_J - \sum_{I,J,K} C_I^*(-H^{\mathrm{el}}_{IJ}X^k_{JK} + X^k_{IJ}H^{\mathrm{el}}_{JK})C_K \qquad (3)$$

associated mass, respectively, and $H^{\mathrm{el}}_{IJ} = \langle \Phi_I | H^{\mathrm{el}} | \Phi_J \rangle$ and $X^k_{IJ} = \langle \Phi_I | \partial\Phi_J/\partial\boldsymbol{R}_k \rangle$. The first term on the right-hand side of Equation (3) represents the quantum average of electronic forces acting on a nucleus, while the other two terms represent nucleus–electron couplings. Nonadiabatic coupling is taken into account by the off-diagonal elements X^k_{IJ} and/or H^{el}_{IJ}. Equations (2) and (3) are integrated with a time step that should be short enough, that is, down to 10 as for the nuclear classical motions and 1 as for the electron quantum wavepacket. Theoretical and computational details are discussed in references [15–17,24].

The low-energy collision of $H_2O + H_3O^+$ begins (at $t = 0$) at an O–O distance of 3.1 Å with a collision energy as low as about $E_{\mathrm{coll}} = 0.027$ eV. The structure and stability of the combined system ($H_2O + H_3O^+$) have been extensively studied.[25–29] The potential energy surface (PES) of the electronic ground state is attractive for formation of $H_5O_2^+$, while the low-lying excited states are repulsive. Another important feature of the PES is that there is no potential barrier and consequently no need to consider quantum tunneling as the first approximation. We set the initial configuration of H_2O and H_3O^+ on a plane for the sake of simple discussions, although the minimum-energy structure of ground-state $H_5O_2^+$ has a skewed geometry.[25–29] Initial geometry and atom labeling are shown in Figure 1. Zero-point vibrational energies for all possible normal modes, including out-of-plane modes, were given to both species, and therefore the planar geometry is relaxed spontaneously during the collision. However, this relaxation is slow, since the energy difference

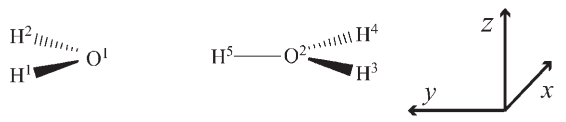

Figure 1. Geometry before collision and labeling of atoms.

---

[*] Dr. H. Ushiyama, Prof. K. Takatsuka
Department of Basic Science
Graduate School of Arts and Sciences
The University of Tokyo
Komaba, 153-8902, Tokyo (Japan)
Fax: (+81) 3-5454-6588
E-mail: kaztak@mns2.c.u-tokyo.ac.jp

[**] The authors thank Dr. Shigeta and Dr. Yagi for their valuable discussions. They are also grateful to one of the referees for valuable comments. This work has been supported in part by a Grant-in-Aid for basic science and the 21st Century COE Program for Frontier in Fundamental Chemistry from the Ministry of Education, Science, Culture, Sports, and Technology of Japan.

between the optimized and in-plane structures is actually very small (ca. 0.1 kcal mol^{-1}), which is less than the vibrational zero-point energy of the corresponding twisting mode (ca. 0.6 kcal mol^{-1}).

The CSFs to expand the electron wavepacket are composed of the Hartree–Fock molecular orbitals, which are generated at each molecular geometry with the STO-6G basis set. The electronic Hamiltonian is represented in terms of the singly and doubly excited configurations within the valence space[15,24] and thus the number of CSFs employed is 861. This is not a state-of-the-art quantum chemical calculation, because of the huge tasks for nuclear coupling along $\boldsymbol{R}(t)$. However, the quality is good enough for qualitative understanding of the reaction mechanisms treated. In what follows, we examine two initial electronic configurations to integrate Equations (2) and (3): the ground state and the first excited state.

Figure 2a shows the time-dependent change in the O^1–H^5, O^2–H^5, and O^1–O^2 distances for the collision starting from the ground state electronic configuration. The decreasing O^1–O^2 distance indicates the approach of two molecules. At about $t = 14.8$ fs, the O^1–H^5 and O^2–H^5 bond lengths interchange, and this defines the instant of H^5 transfer from O^2 to O^1. Herein we study only this first elementary process, although the proton may go back and forth before the entire reaction is over. Figure 2b shows the Mulliken net charges on the $H^1H^2O^1$ and $H^3H^4O^2$ groups, the roles of which interchange smoothly in a synchronous manner with the geometrical change. (Note also the very fast fluctuation in the electronic wavepackets.) In fact, as many as about 0.6 electrons are transferred from the $H^1H^2O^1$ side (neutral H_2O) to the $H^3H^4O^2$ side (oxonium ion before collision). On the other hand, the charge on H^5 remains constant at about +0.4, which implies that the relevant proton is kept covered tightly by about 0.6 electrons, while the net positive charge (+1) must be carried from the oxonium ion to the neutral water molecule. To comprehend all these facts, one can summarize as follows: 1) the proton thus covered is forced to carry as many as about 0.6 electrons, and therefore 2) the same number of electrons should be carried back in the reverse direction by a different path. Therefore this process may be termed "proton transfer with backward electron transfer".

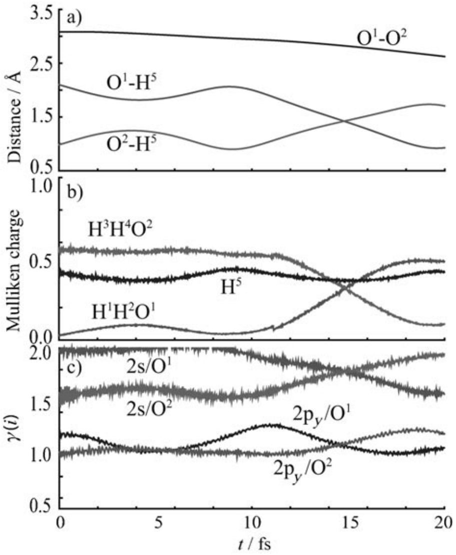

Figure 2. Time-dependent changes of the relevant quantities along the transfer process in the electronic ground state. a) Distances, b) Mulliken charges, and c) the diagonal elements of the electron density matrix based on atomic orbitals, $\gamma(i)$.

We next analyze the pathway and mechanism of the backward electron transfer. First, we note that the norm of the Hartree–Fock ground state configuration, which is the main electronic configuration of this wavepacket, remains almost unity throughout the collision. Therefore, the electron transfer occurred adiabatically. For further information, we examine the electron density matrix (the spinless first-order reduced density matrix[30]) [Eq. (4)], where $g_i(x,y,z,\boldsymbol{R})$ is the

$$\rho(x,y,z) = \sum_{i,j}^{\mathrm{AO}} \gamma_{ij}(\boldsymbol{R}(t)) g_i^*(x,y,z,\boldsymbol{R}) g_j(x,y,z,\boldsymbol{R}) \tag{4}$$

ith atomic orbital centered at a nuclear position $\boldsymbol{R}$. Herein we examine the diagonal matrix elements only. For a simpler notation, we rewrite $\gamma_{ii}(\boldsymbol{R}(t))$ as $\gamma(i)$, and $\gamma(2s/O^1)$ is the electron density of the 2s orbital on the O^1 atom. Figure 2c shows $\gamma(2s/O^1)$, $\gamma(2s/O^2)$, $\gamma(2p_y/O^1)$, and $\gamma(2p_y/O^2)$ as a function of time.

For comparison, Table 1 lists electron populations on the oxygen atoms in the isolated species. Inspection of the densities on H_2O and H_3O^+ suggests that the O^1 atom in H_2O should have hybridization close to sp^3, whereas O^2 in H_3O^+ of planar geometry should have sp^2 hybridization (Figure 3a). The electronic population involved in this sp^2 hybridization is significantly lowered by abstraction toward the additional proton (H^5), but the population in the $2p_z$ orbital is not affected by the additional proton because of the "symmetry". This is the reason why the population in the 2s orbital in H_3O^+ is considerably smaller than that of H_2O. As the proton shifts by breaking the O^2–H^5 bond and forming a new O^1–H^5 bond, their electronic structures exchange their roles smoothly in an adiabatic manner. This pathway of backward electron transfer is visually illustrated in Figure 3.

Table 1: Diagonal elements of the electron density matrix, $\gamma(i)$, on the oxygen atoms of isolated water molecule and oxonium ion.

$\gamma(i)$	H_2O	H_3O^+
2s	2.01	1.53
$2p_x$	0.75	0.98
$2p_y$	1.17	0.98
$2p_z$	2.00	2.00

Next, we examine the dynamics of the colliding system $H_2O + H_3O^+$ in the first excited state. The initial condition for nuclei is chosen to be the same as that for the ground-state dynamics. The electronic configuration examined is shown in Figure 4a. On excitation from the ground to the first excited

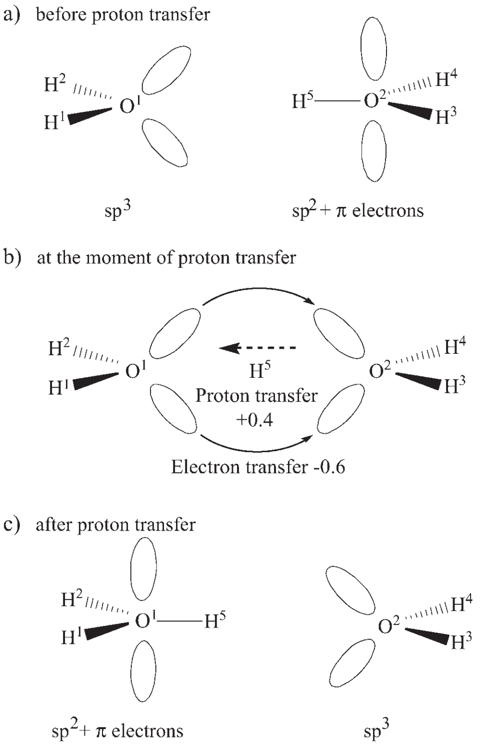

Figure 3. Schematic picture of ground-state electron transfer mediated by alternation of the sp^n hybridization.

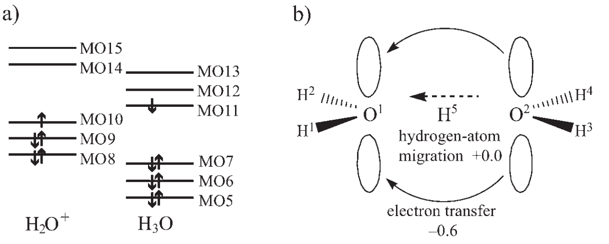

Figure 4. a) The major electronic configuration in the initial first exited state. b) Schematic picture of instantaneous electron transfer in the "π" orbital space.

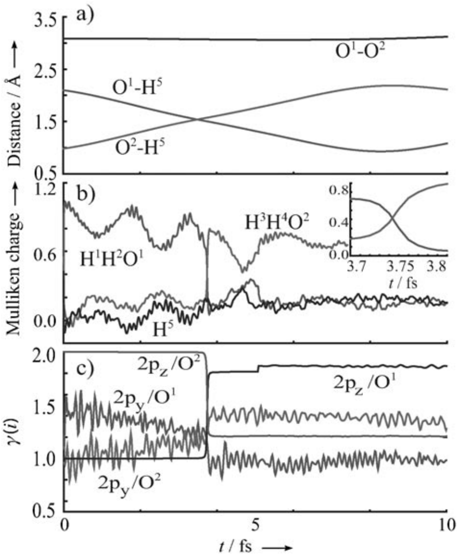

Figure 5. a–c) as in Figure 2, except that the dynamics of the first excited state are monitored. The inset in (b) is a magnification of the electron-transfer region.

state, an electron in $2p_z$ on O^1 (MO 10) is shifted to the LUMO (MO 11), which lies in the molecular plane consisting of antibonding σ interactions between O^2–H^3, O^2–H^4, and O^2–H^5. Therefore, strictly speaking, the system we treat is ($H_2O^+{\cdot}H_3O$). With this initial electronic state, the reaction $H_2O^+ + H_3O \rightarrow H_3O + H_2O^+$ takes place, in which both a hydrogen atom and a single electron are transferred from H_3O to H_2O^+. The relevant geometrical changes, represented by the O^1–H^5, O^2–H^5, and O^1–O^2 distances, are shown in Figure 5a. Since the potential surface is repulsive, mutual approach is very slow. The O^1–O^2 distance becomes shortest at about $t = 6.0$ fs. At about $t = 3.75$ fs, H^5 transfers from O^2 to O^1.

The associated change of the electronic distribution is displayed in Figure 5b. The Mulliken charge on H^5 remains around 0.0 throughout the transfer process. Thus we conclude that this is "hydrogen-atom migration", as opposed to proton transfer in the ground-state dynamics.[18–20] The Mulliken charge on the $H^1H^2O^1$ group jumps from about +0.8 (on average) to about +0.2 (on average) suddenly (during 50–100 as, see the inset of Figure 5b) near the instant of H^5 transfer. On the other hand, the charge on the $H^3H^4O^2$ group also increases suddenly from about +0.2 to +0.8. Thus, electron transfer takes place in the same direction as hydrogen transfer. This may be termed "forward electron transfer with hydrogen-atom migration".

The mechanism of this electron transfer is as follows if we assume an approximate separation of σ and π orbital spaces. The bond rearrangement between O^2–H^5 and O^1–H^5 should be performed within the "σ" orbital space. On the other hand, electron transfer should take place in the "π" orbital space, since the hole in $2p_z/O^1$ has been transferred to $2p_z/O^2$, as shown in Figure 5c. $2p_z/O^1$ and $2p_z/O^2$ are "π" orbitals and correspond to MO 7 of H_3O and MO 10 of H_2O^+, respectively. At the incident of hydrogen-atom migration, the roles of $\gamma(2p_y/O^1)$ and $\gamma(2p_y/O^2)$ are interchanged. This is a reflection of O^2–H^5 bond cleavage and formation of a new O^1–H^5 bond in the "σ" orbital space. However, much larger changes are observed in $\gamma(2p_z/O^1)$ and $\gamma(2p_z/O^2)$. Quantitatively, the amount of exchanged electronic population is roughly 0.6–0.7. Therefore, it is readily concluded that forward electron transfer has taken place in the "π" bond space.

In clear contrast to the smooth adiabatic change in the ground-state dynamics, the first excited-state dynamics describe a nonadiabatic transition, that is, the electron transfer is induced by the nuclear motion. In the terminology of orbital mixing, the mixing coefficient between π_u and π_g has changed abruptly from $\pi_u + \pi_g$ to $\pi_u - \pi_g$ in the electron wavepacket. This scheme is illustrated in Figure 4b. Finally, the observed time required for the sudden electron jump (with an interval of 50–100 as[31]) may give a general time scale for other nonadiabatic electron transfers involved in reactions such as

$K + Br_2 \rightarrow K^+ + Br_2^- \rightarrow KBr + Br$ (the harpoon mechanism, see reference [32]).

We have reported some of the basic mechanisms of electron transfer coupled with proton transfer and hydrogen-atom migration in the prototype system $H_2O + H_3O^+$. Two cases have been studied: 1) proton transfer with simultaneous (adiabatic) backward electron transfer in the electronic ground state, and 2) hydrogen-atom migration with instantaneous (nonadiabatic) forward electron transfer in the first excited state. Nevertheless, there are more types of coupled transfers even in this small system, which are observed in the different excited electronic states. These will be reported elsewhere.[24]

Received: August 31, 2006

Keywords: attochemistry · electron transfer · hydrogen transfer · molecular dynamics · proton transport

[1] V. May, O. Kühn, *Charge and Energy Transfer Dynamics in Molecular Systems*, Wiley-VCH, Berlin, **2000**.
[2] L. I. Krishtalik, *Biochim. Biophys. Acta* **2000**, *1458*, 6–26.
[3] M. R. Gunner, E. Alexov, *Biochim. Biophys. Acta* **2000**, *1458*, 63–87.
[4] M. Y. Okamura, M. L. Paddock, M. S. Graige, G. Feher, *Biochim. Biophys. Acta* **2000**, *1458*, 148–163.
[5] I. Belevich, M. I. Verkhovsky, M. Wikstrom, *Nature* **2006**, *440*, 829–832.
[6] C. Tommos, G. T. Babcock, *Biochim. Biophys. Acta* **2000**, *1458*, 199–219.
[7] K. Nishi, H. Sekiya, H. Kawakami, A. Mori, Y. Nishimura, *J. Chem. Phys.* **1998**, *109*, 1589–1592.
[8] K. Nishi, H. Sekiya, H. Kawakami, A. Mori, Y. Nishimura, *J. Chem. Phys.* **1999**, *111*, 3961–3969.
[9] H. Ushiyama, K. Takatsuka, *Angew. Chem.* **2005**, *117*, 1263–1266; *Angew. Chem. Int. Ed.* **2005**, *44*, 1237–1240.
[10] H. Ushiyama, K. Takatsuka, *J. Chem. Phys.* **2001**, *115*, 5903–5912.
[11] H. Niikura, F. Legare, R. Hasbani, A. D. Bandrauk, M. Y. Ivanov, D. M. Villeneuve, P. B. Corkum, *Nature* **2002**, *417*, 917–922.
[12] J. Itatani, J. Levesque, D. Zeidler, H. Niikura, H. Pepin, J. C. Kieffer, P. B. Corkum, D. M. Villeneuve, *Nature* **2004**, *432*, 867–871.
[13] H. Katsuki, H. Chiba, B. Girard, C. Meier, K. Ohmori, *Science* **2006**, *311*, 1589–1592.
[14] I. Barth, J. Manz, *Angew. Chem.* **2006**, *118*, 3028–3031; *Angew. Chem. Int. Ed.* **2006**, *45*, 2962–2965.
[15] M. Amano, K. Takatsuka, *J. Chem. Phys.* **2005**, *122*, 084113.
[16] K. Yagi, K. Takatsuka, *J. Chem. Phys.* **2005**, *123*, 224103.
[17] K. Takatsuka, *J. Chem. Phys.* **2006**, *124*, 064111.
[18] C. Tanner, C. Manca, S. Leutwyler, *Science* **2003**, *302*, 1736–1739.
[19] W. Domcke, A. L. Sobolewski, *Science* **2003**, *302*, 1693–1694.
[20] A. L. Sobolewski, W. Domcke, *Phys. Chem. Chem. Phys.* **2002**, *4*, 4–10.
[21] J. B. Delos, *Rev. Mod. Phys.* **1981**, 53, 287–357.
[22] J. C. Tully in *Modern Methods for Multidimensional Dynamics Computations in Chemistry* (Ed.: D. L. Thompson), World Scientific, Singapore, **1998**, pp. 34–72.
[23] A. W. Jasper, B. K. Kendrick, C. A. Mead, D. G. Truhlar in *Modern Trends in Chemical Reaction Dynamics* (Eds.: X. Yang, K. Liu), World Scientific, Singapore, **2004**, pp. 329–391.
[24] H. Ushiyama, K. Takatsuka, unpublished results.
[25] M. Tuckerman, K. Laasonen, M. Sprik, M. Parrinello, *J. Chem. Phys.* **1995**, *103*, 150–161.
[26] M. Tuckerman, K. Laasonen, M. Sprik, M. Parrinello, *J. Phys. Chem.* **1995**, 99, 5749–5752.
[27] X. Huang, B. J. Braams, J. M. Bowman, *J. Chem. Phys.* **2005**, *122*, 044308.
[28] J. Rheinecker, T. Xie, J. M. Bowman, *J. Chem. Phys.* **2004**, *120*, 7018–7023.
[29] D. J. Wales, *J. Chem. Phys.* **1999**, *110*, 10403–10409.
[30] A. Szabo, N. E. Ostlund, *Modern Quantum Chemistry*, Dover, New York, **1996**.
[31] The period of the 1s electron of the hydrogen atom is about 152 as in the Bohr model.
[32] R. D. Levine, *Molecular Reaction Dynamics*, Cambridge University Press, Cambridge, UK, **2005**.